Development and characterization of imatinib-loaded PEG-ASA polymeric micelles and co-administration with doxorubicin-loaded micelles.

by

Apurva Rajesh Pardeshi

B. Pharmacy, Institute of Chemical Technology, Mumbai, 2019

Submitted to the Graduate Faculty of the

School of Pharmacy in partial fulfillment

of the requirements for the degree of

Master of Science

University of Pittsburgh

2021

UNIVERSITY OF PITTSBURGH

SCHOOL OF PHARMACY

This thesis/dissertation was presented

by

Apurva Rajesh Pardeshi

It was defended on

March 30, 2021

and approved by

Dr. Song Li, Professor, Pharmaceutical Science

Dr. Xiaochao Ma, Associate Professor, Pharmaceutical Science

Dr. Jingjing Sun, Research Instructor, Pharmaceutical Science

Thesis Advisor/Dissertation Director: Dr. Song Li, Professor, Pharmaceutical Science

Development and characterization of imatinib-loaded PEG-ASA polymeric micelles and co-administration with doxorubicin-loaded micelles.

Apurva Rajesh Pardeshi, B. Pharm.,

University of Pittsburgh, 2021

Imatinib is a tyrosine kinase inhibitor widely used in the treatment of chronic myeloid leukemia and gastrointestinal stromal tumors. Monotherapy with imatinib (IMA) can lead to resistance, toxicity, and related side effects. Using polymeric micelles to facilitate its targeted delivery to tumor tissues reduces systemic toxicity and helps to reduce rapid metabolism and renal clearance along with increasing drug accumulation in tumor tissue due to enhanced permeation and retention effect. COX2 plays a role in tumor cell proliferation, angiogenesis, inhibition of apoptosis, and immunosuppression. Its inhibition can thus lead to increased anti-tumor activity. 5-ASA is a known anti-inflammatory COX2 inhibitor and can be conjugated with a polymer to form a prodrug-based micellar carrier to load other chemotherapeutic agents. PEG-ASA polymer (PASA) was hence synthesized and used to load imatinib to form polymeric micelles. These micelles were then characterized for their size, morphology, as well as *in vitro* and *in vivo* anti-tumor efficacy. We further developed doxorubicin (DOX)-loaded PASA micelles and tested their combination effect with co-administration of imatinib-loaded PASA micelles.

Our studies demonstrated that combination of IMA- and DOX-loaded micelles showed a favorable anti-tumor efficacy in *in vitro* as well as *in vivo* studies and may represent a promising therapeutic strategy that warrants more studies in the future.

Table of Contents

List of Tables

List of Figures

List of Schemes

1.0 Introduction

1.1 Imatinib and its chemotherapeutic activity

Imatinib belongs to the family of tyrosine kinase inhibitory (TKI) drugs that inhibit protein tyrosine phosphorylation, that is, the transfer of the terminal phosphate from ATP to the tyrosine residues on its substrates[1,2]. Such an activity has a detrimental effect on all the downstream pathways that lead to tumor proliferation and the inhibition of apoptosis. Imatinib is known to be particularly active against KIT, PDGFRA, ABL and BCR-ABL oncoproteins[3-5]. It is widely used for the treatment of chronic myeloid leukemia and gastrointestinal stromal tumors and demonstrates a superior chemotherapeutic activity by inducing an effective clinical response as well as increasing the overall survival for majority of the patients[6,7].

1.1.1 Immunomodulatory effects of imatinib

TKIs are known to exhibit immunomodulatory effects. In certain studies, imatinib and sunitinib have shown to have an inhibitory effect on the population of myeloid derived suppressor cells (MDSC) in the tumor microenvironment. MDSC's are responsible for suppressing tumor immune responses by many pathways including the induction of regulatory T cells that in turn are known to have a deleterious effect on functional immune cells like effector T cells, natural killer cells, dendritic cells, and B cells[8,9]. By decreasing the number of MDSC's, imatinib can hence enhance tumor immune responses. Imatinib is also reported to enhance the $CD8^+$ T cell response

and decrease the T_{reg} cell population in the tumor microenvironment directly[10,11]. Hence, these attributes of imatinib can be explored in order to obtain a robust cytotoxic immune response.

1.1.2 Limitation of imatinib therapy

Although it has been shown to have an effective anti-tumor activity, various studies have reported that imatinib therapy alone is almost never curative due to the development of resistance in patients after long term therapy[12,13]. This resistance can be attributed to various factors such as introduction of mutations as well as overexpression of various members of the ATP binding cassette proteins[14]. In order to overcome the issue of resistance developed due to imatinib monotherapy, combination therapy with another chemotherapeutic drug or immunotherapy can be adopted to obtain a better therapeutic outcome[15].

1.2 Advantages of combination therapy

Synergistic combinations of imatinib therapy with either other chemotherapeutic drugs or immunotherapy can not only help to overcome resistance to imatinib monotherapy but also help to reduce chances of toxicity and adverse effects associated with monotherapy[16,17]. Since two or more drugs or therapeutic routes are used, their synergistic action aiming at two or more different targets helps to reduce the dose of an individual agent hence reducing chances of systemic toxicity. Such a strategy can also help to reduce incidences of relapses and keeps a check on tumor metastasis.

1.2.1 Use of doxorubicin for combination therapy with imatinib.

DOX is a highly potent chemotherapeutic drug known for its effective anti-tumor activity against multiple types of cancers. It exerts its cytotoxic activity at the nuclear level by intercalating with the DNA and causing significant DNA damage which in turn affects the macromolecular synthesis and thus tumor cell proliferation. Similar to the case of IMA, monotherapy with DOX has not shown favorable outcomes due to development of multi-drug resistance and low cytotoxic activity even at a high concentration[18]. DOX is also known to cause systemic toxicity including serious cardiotoxic and nephrotoxic reactions[17,19].

Hence, combination therapy with DOX and IMA can help to overcome the disadvantages posed by monotherapy with both these drugs and display an efficient anti-tumor activity.

1.3 COX inhibition and anti-tumor activity

Various studies have demonstrated a relationship between COX2 expression and tumor proliferation. The tumor microenvironment is infiltrated with various kinds of cytokine-producing immune cells which in turn lead to chronic inflammation[20]. COX2 is known to enhance tumor proliferation by supporting angiogenesis and inhibition of apoptosis in addition to having a suppressive effect on anti-tumor immunity. Overexpression of COX2 has also been shown to be involved in the development of resistance to imatinib therapy in patients[21,22]. Since COX2 has protumor properties, studies have been carried out to determine the anti-tumor efficacy of COX2 inhibitors used alone or in combination with other chemotherapeutic agents. Various COX2 inhibitors such as celecoxib have been successfully shown to reverse resistance to imatinib therapy

and induce apoptosis in imatinib resistant cells when treated with a combination of celecoxib and imatinib[23]. Studies have also been carried out depicting that COX2 knockout models show lower tumor weights as compared to their control counterparts as well as show a better immune cell profile in the tumor microenvironment[24,25]. Hence, COX2 inhibition can be considered as an efficient strategy to inhibit tumor cell proliferation.

1.4 Aims and hypothesis.

Considering the effect of COX2 inhibition on tumor microenvironment, a 5-ASA prodrug-based polymer was developed in the lab. 5-ASA is an anti-inflammatory COX2 inhibitor[26] which when conjugated to a PEG-based polymer can act as a prodrug that is released at the target site to exercise its COX2 inhibitory effects. Due to the structural attributes of this system, various hydrophobic drugs can be incorporated into this polymeric nanocarrier. DOX was loaded onto this carrier and these micelles were decorated with folic acid that acted as a targeting ligand to target specific tumor cells overexpressing the folate receptor and hence increasing the effectivity of the formulation[27]. We have followed a similar approach to incorporate imatinib in this polymeric carrier. Imatinib, being a small molecule drug with the presence of amine groups, can be easily loaded onto this polymer to form small sized nanoparticles. We hypothesized the combined therapy with DOX- and IMA-loaded micelles could help to deliver a favorable chemotherapeutic outcome and overcome the disadvantages posed by monotherapy.

2.0 Materials and methods

2.1 Materials

2.1.1 Reagents

DOX.HCL and IMA were obtained from LC Laboratories (MA, USA). 5-ASA was purchased from Frontier Scientific (UT, USA). 4-Cyano-4[(dodecylsulfanylthiocarbonyl)sulfanyl] pentanoic acid (RAFT), 2-Azobis-(isobutyronitrile) (AIBN), poly(ethylene glycol) methacrylate (Mol. Wt.-950, PEG_{950}), 3-(4,5-dimethylthiazol-2-yl)-2,5-diphenyl tetrazolium bromide (MTT) and Dulbecco's Modified Eagle's Medium (DMEM) were bought from Sigma-Aldrich (MO, USA). Anhydrous alcohol was used to recrystallize and purify AIBN. *N*-Succinimidyl Methacrylate (NHS) was purchased from TCI (USA). Roswell Park Memorial Institute (RPMI)-1640 medium, fetal bovine serum (FBS) and penicillin-streptomycin solution were bought from Invitrogen (NY,USA). HPLC grade solvents were used for all the experiments in this study.

2.1.2 Cell lines

All cell lines used in this study were obtained from ATCC (Manassas, VA). CT26 murine colon cancer cells were cultured in RPMI-1640 medium supplemented with 10% FBS and 1% penicillin-streptomycin whereas MC38 murine colon cancer cells were maintained in a similarly supplemented DMEM medium. All cell cultures were maintained in humidified conditions at 37°C under 5% CO_2.

2.1.3 Animals

Female BALB/c mice (4-6 weeks) were obtained from The Jackson Laboratory (ME, USA). These animals were housed in accordance with AAALAC (Association for Assessment and Accreditation of Laboratory Animal Care) guidelines under pathogen free conditions. All in-vivo experiments pertaining to this study were carried out in complete compliance with institutional guidelines and were approved by the Animal Use and Care Administrative Advisory Committee at the University of Pittsburgh.

2.2 Synthetic Schemes

2.2.1 Synthesis of PEG-*b*-PNHS

Three separate batches of PEG-*b*-PNHS were prepared with different ratios of PEG_{950} to NHS. The different concentrations of materials used for the syntheses are shown in Table 1. 4-Cyano-4[(dodecylsulfanylthiocarbonyl)sulfanyl] pentanoic acid, AIBN, NHS and PEG_{950} were mixed with 2 ml of dried tetrahydrofuran in a schlenk tube in the presence of N_2 to eliminate the oxygen dissolved in the reaction mixture. This was further achieved by following a designated freeze-pump-thawing method. The reaction mixture was frozen using liquid N_2 under vacuum for 5 min followed by melting under N_2 flow at room temperature. This cycle was repeated thrice, and the mixture was allowed to react at 84°C overnight under constant stirring and N_2 flow. Once the reaction was complete, the reaction mixture was precipitated with the help of three consequent

diethyl ether washes on the following day. The solid precipitate of PEG-*b*-PNHS was then collected, dried in a vacuum pump, and structurally confirmed with proton NMR analysis.

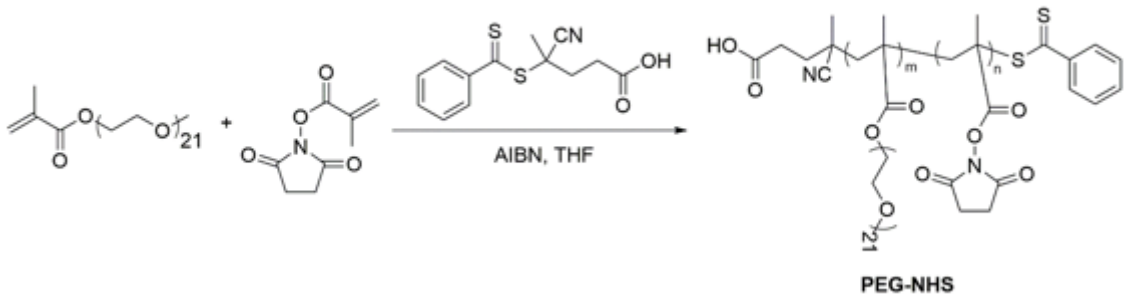

Scheme 1: Synthesis of PEG-b-PNHS

2.2.2 Synthesis of PASA polymer

All the batches of PEG-*b*-PNHS were dissolved with the required quantities 5-ASA (3 times the molar quantity of NHS) and TEA (10 times the molar concentration of NHS) in sufficient volume of DMSO and allowed to react at 37°C under constant stirring at 300rpm for 72hrs (Table 1). On completion, the reaction mixture was dialyzed against DMSO for 2 days followed by dialysis in water for 3 days at room temperature. The obtained solution was then filtered, frozen at -80°C and lyophilized until solid polymer is obtained. The polymer solution was prepared in a 1:1(v/v) mixture of dichloromethane (DCM) and methanol.

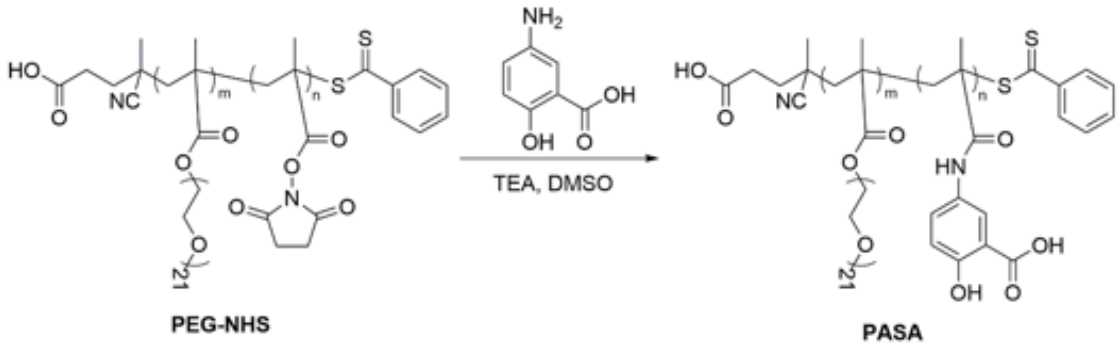

Scheme 2: Synthesis of PASA polymer

Table 1: Materials for synthesis of PASA polymer

PEG:NHS	PEG_{950} (mg)	NHS(mg)	RAFT reagent(mg)	AIBN(mg)	5-ASA(g)	TEA(ml)
1:6	350	404.53	10.2	2	1	3.08
1:7	350	471.95	10.2	2	1.177	3.595
1:8	350	539.37	10.2	2	1.345	4.108

2.2.3 Chemical characterization of synthesized polymer

The final PASA polymer was dissolved in DMSO-d_6 and its ^{1}H-NMR spectrum was obtained using a Varian-400 FT-NMR spectrometer at 400.0 MHz.

2.3 Preparation of Blank, DOX-loaded, and IMA-loaded micelles.

Film hydration method was used to prepare all micelles. IMA and DOX stock solutions were prepared in a 1:1 (v/v) mixture of DCM and methanol. 5 molar equivalent of TEA was additionally added to the DOX stock solution to remove HCl. Suitable volumes of these drug stock solutions were mixed with calculated amounts of polymer solutions according to different drug: polymer weight ratios. The final solution was air-dried to form a uniform thin film. These samples were further kept under vacuum for 2hrs to eliminate the remaining solvent. The film was then hydrated using freshly prepared PBS and samples were agitated gently to obtain drug loaded micelles. Blank micelles were prepared similarly without the addition of drug stock solutions.

2.4 Characterization of micelles

Dynamic light scattering (DLS) method was used to evaluate the size distribution of micelles filtered through 0.22µm filter using zetasizer software. Further, diluted samples of micelles were evaluated for their morphology by visualization under transmission electron microscopy (TEM). Negative staining technique was used for the TEM which enhances the contrast and enables visualization of the micelles at a higher resolution. The concentration of IMA loaded in micelles was evaluated by breaking the micelle structure by dissolution in methanol after they had been dialyzed over 2 nights to eliminate presence of free drug. The methanol-dissolved samples were further filtered through a 22µm filter and analyzed by waters e2695 HPLC system equipped with a Waters 2489 UV detector. The mobile phase used for the analysis consisted of solvent A as water with 0.1% formic acid and solvent B as acetonitrile (ACN) with 0.1% formic

acid. The ratio of solvent A to B used was 90:10 with a flow rate of 1ml/min and UV absorption at 268nm. The standard solutions of the various concentrations of the drug for the calibration curve were made in methanol. The drug loading capacity and the drug loading efficiency for the micelles were then calculated based on the following equations:

$$DLC(\%) = \left[\frac{Weight\ of\ loaded\ drug}{(weight\ of\ polymer + input\ drug)}\right] \times 100\%$$

$$DLE(\%) = \left(\frac{weight\ of\ loaded\ drug}{weight\ of\ input\ drug}\right) \times 100\%$$

The colloidal stability studies were carried out with multiple micelle samples and their size uniformity and appearance for any precipitates were observed at various decided time points at every hour after preparation until 12hrs followed by daily monitoring for a week.

2.5 *In vitro* cytotoxicity assay

Cytotoxicity assays were performed aimed at 2 endpoints. One was to determine the effect of the combination of IMA and 5-ASA and their synergistic anti-tumor activity *in vitro* if any; the second was to determine the antitumor efficacy of DOX and IMA free drugs and free drug combinations as well as the activity of IMA and DOX loaded micelles when used alone and in combination. Two cancer cell lines CT26 and MC38; which are murine colon cancer cell lines; were used for these assays. 96-well plates were seeded with these cells at a density of 3000 cells/well with 100µl of media (DMEM or RPMI-1640) supplemented with 10% FBS and 1% streptomycin/penicillin and cultured overnight under 5% CO_2 at 37°C.

To determine the combination effect of IMA and 5-ASA, cells were treated with various concentrations of free IMA, 5-ASA and the combination. After a 48hr incubation, the media in the

wells was replaced by 100µl MTT reagent. Following a 4hr incubation, the MTT reagent was replaced with 100µl of DMSO in order to dissolve the formazan crystals leading to the formation of a purple-colored solution. The absorbance of each plate was measured at 590nm by a UV spectrophotometer and the cell viability was calculated using the given formula:

$$Cell\ viability(\%) = \left(\frac{OD_{treated} - OD_{blank}}{OD_{control} - OD_{blank}}\right) \times 100\%$$

The anti-tumor activity of DOX loaded PASA and IMA loaded PASA at a drug:polymer ratio of 1:10 and their combination effect was compared to free DOX, IMA, and their combination at various drug concentrations. Blank PASA micelles were used as control with the polymer concentration equivalent to the amount of polymer used in the corresponding drug loaded micelle formulations. The MTT assay was carried out in a similar way after a 48hr incubation.

2.6 *In vivo* therapeutic efficacy study

Two *in vivo* studies were carried out. The first was a preliminary study carried out to determine and optimize the dose of IMA to be administered to the mice in order to obtain a favorable anti-tumor response and for use in all further studies whereas the second study was carried out in order to determine the exact anti-tumor efficacy of the drug loaded micelle systems and their combination therapy. All the studies were carried out in CT26 mouse colon cancer models. 4-6 weeks old female BALB/c mice were inoculated with 5×10^5 tumor cells/mouse subcutaneously. When the tumor volume reached to about 50 mm^3, the mice were divided in a random manner into 4 groups.

For the preliminary study, mice were treated via tail vein injection with PBS (Group 1) and PASA/IMA (drug:polymer ratio of 1:10) with IMA loaded at different doses of 5mg/kg (Group 2), 10mg/kg (Group 3) and 20mg/kg (Group 4) with 3 mice per group. These mice were administered with a total of 5 injections spaced at 1 injection in 3 days.

For the second study carried out in order to determine the anti-tumor efficacy of IMA loaded micelles and their synergistic efficacy when used in combination with DOX loaded micelles, mice were injected with PBS (Group1), PASA/DOX (Group 2), PASA/IMA (Group 3) and a combination of PASA/DOX and PASA/IMA. The drug:polymer ratio for all micelles was 1:10 and dose used for both drugs was 5mg/kg. Each group consisted of five mice that were injected with the respective formulation for 3 injections for PASA/DOX and 5 injections for PASA/IMA once in three days. For group 4, PASA/DOX was injected on day 1 followed by PASA/IMA injection on the consecutive day.

During both these studies, tumor volumes were closely monitored by measuring tumor dimensions every three days starting from the first day of injection. The tumor volume was calculated by using the formula:

$$Tumor\ volume = \frac{length \times width^2}{2}$$

The body weights of the mice were also monitored throughout the course of the study in order to determine if the therapy had any detrimental effects or systemic toxicity in the study mice. After completion of the studies, tumor tissues were harvested and stored under -80°C conditions in order to carry out any further experiments.

2.7 Determination of COX2 expression *in vitro* and *in vivo*.

The expression of COX2 on treatment with various free drugs and drug loaded micelle formulations and their combinations was determined in the CT26 cell line as well as the tumor tissues collected from the *in vivo* studies at the mRNA as well as protein levels. CT26 cells were seeded in 6-well plates at the density of 3×10^5 cells/well in completely supplemented RPMI-1640 medium and cultured overnight at 37°C. Cells were treated with various concentrations of the drug on the next day. After a 24hr incubation, their mRNA was isolated using TRIzol reagent. It was further purified, quantified and reverse transcribed to obtain corresponding cDNA. qPCR was carried out to determine the mRNA expression of COX2 in the treated cell lines.

For determination of COX2 mRNA expression in the tumor tissues collected from the animal-based studies, tumor tissues were homogenized in TRIzol and supernatants are used after centrifugation to obtain mRNA which is processed as described earlier.

The COX2 protein expression in the cell line as well as the tumor tissues was also determined by a western blot analysis. For *in vitro* samples, 3×10^5 CT26 cells were seeded per well in 6-well plates and cultured overnight. Various concentrations of DOX and IMA were added to the cells on the following day. After a 48hr incubation, cells were washed with PBS twice and proteins were extracted from the cells by incubation in PierceTM RIPA buffer at 4°C for 30min. For *in vivo* samples, tumor tissues were homogenized in RIPA buffer to extract the proteins. Protein concentrations were determined by measuring absorbance using BCA method and equivalent concentrations of protein lysate were resolved on a 10% SDS-PAGE based on their molecular weight. Proteins separated on the gel were transferred to a PVDF membrane which was then neutralized by incubation in 5% BSA in PBST for 1hr. The membrane was then incubated with COX2 primary antibody at 4°C overnight. The membrane was washed thrice with PBST

followed by a 1hr incubation with goat antirabbit IgG secondary antibody at room temperature. The proteins present on the membrane were then visualized by chemiluminescence detection with cyclophilin B as loading control.

2.8 Quantification of tumor-infiltrating immune cells

Mice were inoculated with CT26 tumors and randomly divided into 5 groups with 3 mice each after the tumors reached a volume of about 50 mm^3. Mice were then administered with PBS (Group 1), blank PASA (Group 2), PASA/DOX (Group 3), PASA/IMA (Group 4) and a combination of PASA/DOX and PASA/IMA (Group 5) at drug dose of 5mg/kg and drug:polymer ratio of 1:10 via tail vein injection. A total of 3 injections were spaced 4 days apart and the PASA/IMA injection for the combination group (Group 5) was administered one day after the PASA/DOX injection. Mice were sacrificed 24hrs after the last injection and their tumors and spleens were harvested. Single cell suspensions were prepared and stained for various markers for flow cytometry analysis.

2.9 Statistical Analysis

All studies were analyzed by GraphPad Prism 8 and values are reported as mean ± standard error of mean (SEM). Student's *t*-test was used to carry out statistical analysis for comparison between two groups whereas comparison between multiple groups was carried out by one-way analysis of variance (ANOVA). Statistical significance was considered if $p < 0.05$.

3.0 Results

3.1 Micelle characterization

3.1.1 Synthesis of the PASA polymer

Scheme 1 and scheme 2 depict the synthesis route of the PASA polymer. Reversible addition-fragmentation chain-transfer (RAFT) polymerization was used to facilitate the reaction of PEG_{950} with *N*-Succinimidyl methacrylate in order to obtain PEG-*b*-PNHS. At a high temperature (84ºC), AIBN acted as an initiator for the RAFT reaction and monomers were then reacted to form a polymer chain (Scheme 1). A conjugation reaction then led to the coupling of 5-ASA to the PEG-*b*-PNHS to produce PASA. The amine group of the 5-ASA reacts with the NHS ester to form an amide bond eliminating an NHS leaving group to form the final polymer. (Scheme 2).

The polymer was structurally analyzed by examining the ^{1}H-NMR peaks for all the major groups. This analysis also confirmed the extent of conjugation of 5-ASA and hence the ratio of PEG_{950} to 5-ASA.

3.1.2 Physicochemical characterization of Blank, IMA and DOX loaded micelles.

PASA being an amphiphilic molecule can efficiently self-assemble to form small-sized micelles that have the ability to load other hydrophobic drugs. Hence a 5-ASA conjugated polymer can act as a prodrug-based carrier and this system can enable the codelivery of 5-ASA with other

chemotherapeutic drugs. Table 2 shows the size distribution for blank micelles prepared from all the three polymers synthesized with different PEG:ASA ratios. The polymer with PEG:ASA ratio of 1:6 showed the most favorable size characteristic of 112-118 nm.

Further, IMA and DOX were loaded onto the carrier at various drug:polymer weight ratios and the size characteristics of these drug-loaded micelles were documented as shown in table 3. It was observed that the size of the micelles considerably decreased after incorporation of the drug. These micelle sizes followed a decreasing trend with increasing polymer fraction in the system. Both IMA and DOX loaded micelles showed ideal size characteristics at the drug:polymer ratio of 1:10 with IMA loaded micelles ranging from 38 to 52 nm and DOX loaded micelles from 85-89 nm in size when prepared with polymer with a PEG:ASA ratio of 1:6.

The micelles remained stable when dispersed in PBS with no visible precipitates and a uniform size distribution as observed by a colloidal stability study for a period of one week.

Table 2: Size characterization of blank micelles

Batch	PEG:ASA ratio	Blank polymer size (nm)
I	1:6	112-118
II	1:7	125-135
III	1:8	120-151

Table 3: Size distribution of IMA and DOX loaded micelles

Drug:Polymer	P1 (1:6)		P2 (1:7)		P3 (1:8)	
	IMA	DOX	IMA	DOX	IMA	DOX
1:1	108-155	196-222	121-134	157-209	133-144	111-120
1:2	51-54	83-98	92-97	77-89	113-116	99-112
1:5	34-39	69-89	136-156	113-125	151-154	111-120
1:10	38-52	85-89	170-213	123-136	129-162	117-183
1:20	54-61	148-168	74-108	114-134	60-64	94-115

The morphological characteristics of the blank, IMA and DOX loaded micelles as determined by visualization under transmission electron microscopy showed spherical, uniformly distributed micelles as seen in figure 1.

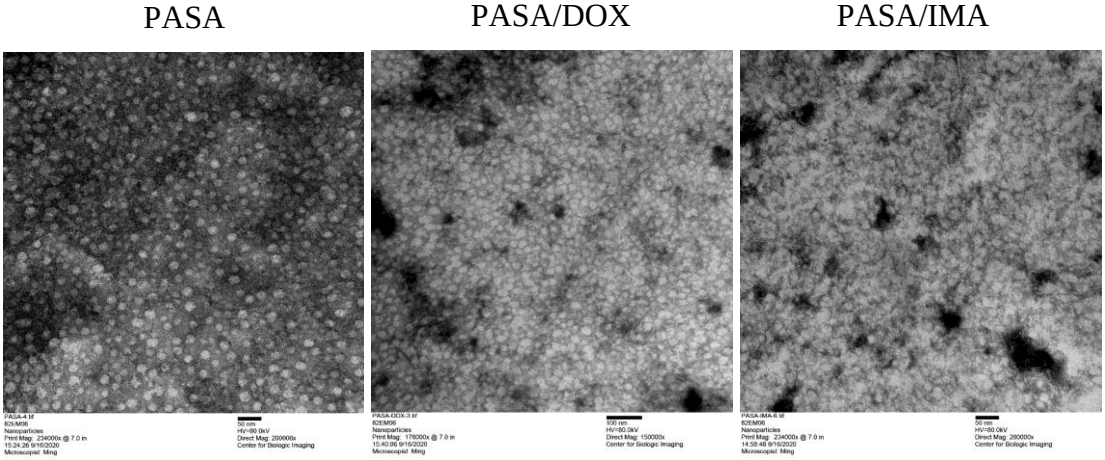

Figure 1: Morpological characteristics of Micelles (TEM)

HPLC analysis to determine the DLC and DLE of micelles prepared at various drug:polymer ratios showed that at the ratio of 1:10, the micelles showed efficient DLE and DLC

of 80.5% and 7.32% respectively. Based on the micelle characteristics, it was decided that since micelles made with polymer having the PEG:ASA ratio of 1:6 and at drug:polymer ratio of 1:10 show ideal characteristics; micelles with these specifications will be used for all the further studies.

Table 4: DLC and DLE characteristics of micelles

Drug:Polymer ratio	Drug loading efficiency (%)	Drug loading capacity (%)
1:2	19.37	6.46
1:5	37.47	6.25
1:10	80.5	7.32
1:20	109.24	5.20

3.2 *In vitro* cytotoxicity assay

3.2.1 Cytotoxicity of 5-ASA, alone or in combination with IMA in CT26 and MC38 cell lines

An MTT assay was used to determine the cell viability after treatment with various treatment groups. This assay helps to determine the cell viability by evaluating the extent of reduction of tetrazolium salts (MTT reagent) by the cells. Oxidoreductase enzymes present in metabolically active cells reduce yellow MTT to purple formazan. These formazan crystals when dissolved in DMSO, form a uniformly purple colored solution. Spectrophotometric analysis of the solution in the wells indicates the cell viability. A darker solution indicates a higher concentration of formazan produced, in turn indicating that a higher number of viable cells were present in the well.

Figure 2 shows the *in vitro* cytotoxicity observed in cell lines when treated with 5-ASA and IMA free drugs as well as a combination of both drugs. Cells were treated with 5-ASA over a range of 0-1mM and it was observed that free 5-ASA does not have any significant anti-tumor activity *in-vitro* and co-treatment of cells with 5-ASA also does not improve the efficiency of the cytotoxic activity of IMA. IMA showcases its antitumor effect in a dose dependent manner as cell viability was seen to decrease with increasing doses of IMA. Previous studies have reported that COX inhibition could have an anti-tumor effect *in vivo* either alone or in combination with therapy with another chemotherapeutic. This could be attributed to the significance of COX inhibition in the tumor microenvironment and its cytotoxic effect that may not be applicable to the *in-vitro* study conditions.

Hence further *in vivo* studies were carried out to confirm this using IMA loaded polymeric micelles prepared with a 5-ASA prodrug-based PASA polymer. This system was used to determine if 5-ASA had any anti-tumor activity *in vivo* when used alone or in combination with IMA.

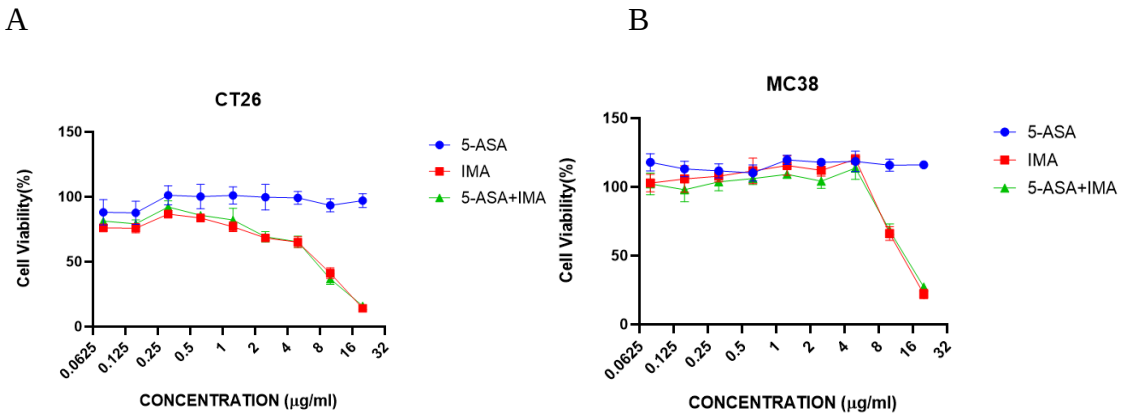

Figure 2: Proliferation inhibition on treatment with a combination of IMA and 5-ASA in (A) CT26 and (B) MC38 cell lines

3.2.2 Cytotoxicity of IMA loaded PASA micelles and their combination with DOX loaded PASA micelles.

Another MTT study was employed to the determine the cytotoxic activity of DOX and IMA free drugs and their combination as well PASA, PASA/IMA and PASA/DOX used alone and in combination. It was observed that IMA and DOX free drugs have a dose-dependent cytotoxicity which is enhanced with combined therapy of the free drugs in both CT26 as well as MC 38 cell lines (Figure 3. A,B). When the cytotoxic activity of blank and drug loaded micelles was evaluated, it was found that PASA alone did not have a significant anti-tumor activity even at the highest concentration. PASA/IMA and PASA/DOX have significant antitumor activity when used alone with PASA/DOX faring better than PASA/IMA. Combined therapy with PASA/DOX and PASA/IMA showed superior anti-tumor activity as compared to all other groups (Figure 3. C,D).

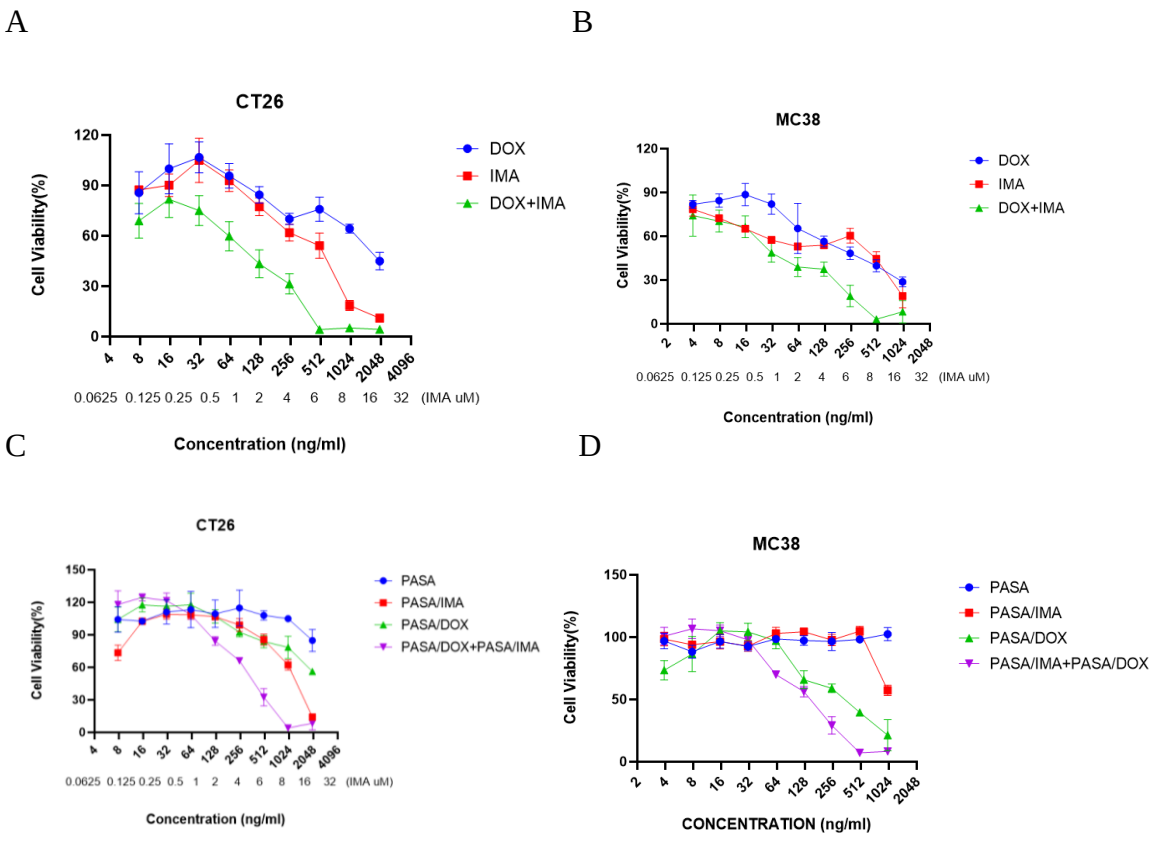

Figure 3: Cytotoxicity assay for free drugs IMA and DOX in (A) CT26 and (B) MC38 cell lines and IMA loaded micelles and their combination with DOX loaded micelles in (C) CT26 and (D) MC38 cell lines

3.3 *In vivo* anti-tumor efficacy study

The CT26 murine colon cancer model was used to determine the anti-tumor activity of the proposed system. After tumor inoculation, when the tumors reached a particular size and volume, injections of respective formulations were administered to the mice via tail vein injection. For the preliminary study conducted to determine the IMA dosage to be used for the consequent studies, mice were treated with three different doses of IMA ranging from 0-20mg/kg. Saline was injected for the control group to mimic normal tumor growth conditions. Tumor volumes were measured

throughout the period of the treatment and relative tumor volumes were plotted. The relative tumor volume was calculated as

$$Relative\ tumor\ volume = \frac{Volume\ at\ a\ given\ time\ point}{Initial\ tumor\ volume\ before\ 1^{st}\ injection}$$

A significant anti-tumor activity was observed at all the IMA doses with the highest dose of 20mg/kg showing the best cytotoxic activity and 5 and 10mg/kg showing almost similar anti-tumor efficacy (Figure 4 A). The body weights of the mice were also monitored and since there was no significant decrease in the body weight, it was deduced that these concentrations of IMA did not lead to any systemic toxicity (Figure 4 B).

Since a significant anti-tumor activity was observed with a dose of 5mg/kg (Figure 4 A), this dose of IMA was used for the subsequent *in vivo* therapeutic study taking into consideration that the following study would consist of combination treatment with two drugs and although safe with monotherapy, a higher dose of IMA could lead to increased toxicity with dual therapy.

A B

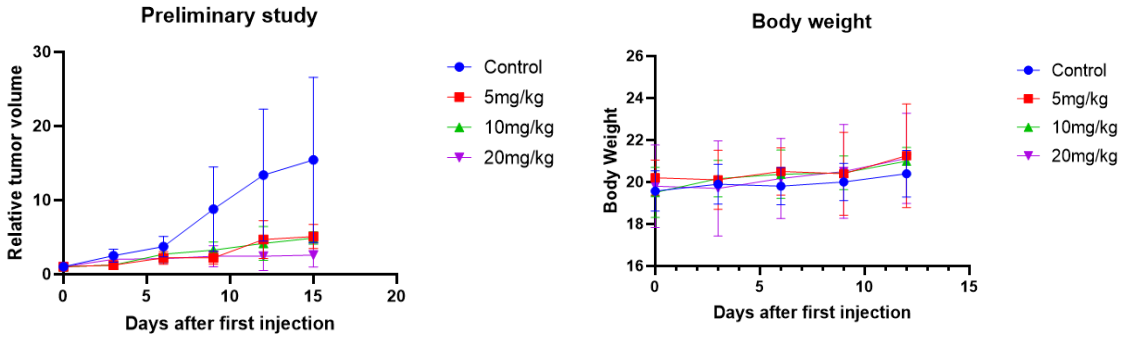

Figure 4: Preliminary *in vivo* therapeutic study (A) relative tumor volume (B) body weight

A following *in vivo* study was conducted to determine the anti-tumor efficacy of PASA/IMA and its combination with PASA/DOX. Mice with sufficiently grown tumors were then divided into 4 groups and treated with Saline, PASA/DOX, PASA/IMA and a combination of

PASA/DOX and PASA/IMA with DOX and IMA dose at 5mg/kg for 3 PASA/DOX injections and 5 PASA/IMA injections spaced 3 days apart. For the combination group, PASA/IMA was injected on the day following the PASA/DOX injection. Relative tumor volumes were calculated as previously described and plotted into a growth curve (Figure 5 A). It was observed that PASA/IMA and PASA/DOX had significant anti-tumor efficacy as the tumor volumes significantly reduced over the period of treatment. Although PASA/DOX showed a better anti-tumor profile as compared to PASA/IMA alone, the anti-tumor efficacy observed in the combination group was superior as compared to individual therapy groups. Combination of PASA/DOX and PASA/IMA showed a significant reduction in the tumor volume especially following the last two PASA/IMA injections. Even though the body weights of the mice in the combination group showed a slight decrease around the 10-12 day, they regained the weight around day 15 and hence it was observed that the body weights were not significantly affected by the combination therapy indicating that the therapeutic conditions did not lead to any toxicity in these mice (Figure 5 B).

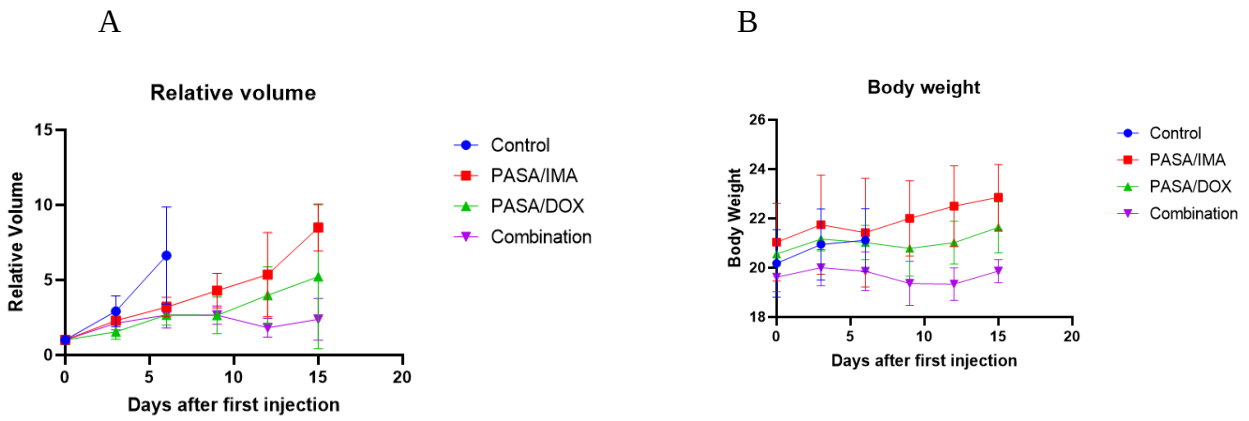

Figure 5: *In vivo* therapeutic efficacy of combination treatment (A) relative tumor volume (B) body weight

3.4 Determination of COX2 expression *in vitro* and *in vivo*

qPCR analysis was carried out to determine the mRNA expression of COX2 in CT26 cell line after treatment with various concentrations of DOX. Expression was also determined in tumor tissues harvested from the *in vivo* study after treatment with various formulations. As shown in Figure 6 A, it was observed that the COX2 mRNA expression significantly decreased on exposure to increased concentrations of DOX as compared to the basal expression. This was similarly reflected in the western blot results showing a dose-dependent decrease in the COX2 level on treatment with DOX (Figure 6 B).

In the tumor tissues collected from the *in vivo* study, it was evident that on treatment with PASA, PASA/DOX, PASA/IMA and a combination of PASA/DOX and PASA/IMA, the COX2 mRNA expression decreased significantly as compared to the basal mRNA expression. The most significant decrease was seen in the group treated with the combination of drug-loaded micelles followed by PASA/DOX group (Figure 6 C). This decrease can be attributed to the *in vivo* COX inhibitory effect of the 5-ASA based polymer PASA acting in the tumor microenvironment. The western blot study carried out to determine the COX2 protein levels in the *in vivo* samples showed a varied result. This can be attributed to the presence of various different cell types and their functionality in the tumor microenvironment. The levels of COX2 can be influenced by contributions from other immune cells and stromal cells present in and around the tumor tissues.

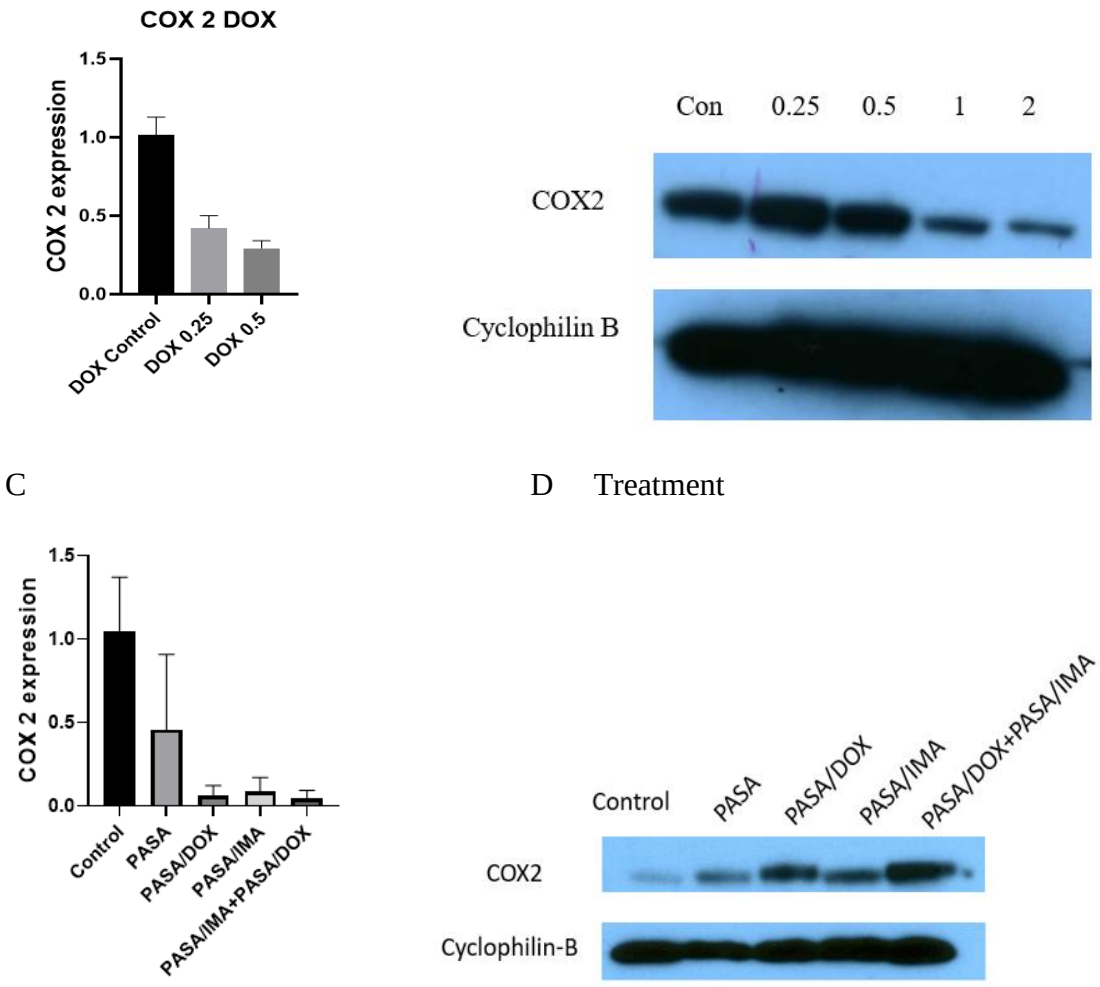

Figure 6: COX2 mRNA and protein expression (A) and (B) CT26 cell line, (C) and (D) CT26 Tumor tissues

3.5 Determination of tumor infiltrating immune cells.

An *in vivo* study was carried out in order to determine the effect of various treatments on the tumor immune microenvironment. IMA is known to support the induction and increase in the population of $CD8^+$ T cells as well as their proliferation in the tumor microenvironment[3]. Although the number of $CD8^+$ and $CD4^+$ T cells are not affected significantly by the treatment with various

formulations administered (Figure 7. A,B), it was observed that the IFNγ$^+$ CD4$^+$ T cells as well as IFNγ$^+$ CD8$^+$ T cells were significantly increased after treatment with the various micelle formulations as compared to control (Figure 7. D,E). Increased levels of IFNγ indicate T cell activation[28]. Hence such an increase shows an increase in functional T cells. It was also observed that GzmB$^+$ CD8$^+$ T cells were increased in the treatment groups as compared to the control especially in the combination group followed by the PASA/DOX group (Figure 7. F). T_{reg} cells have been known to demonstrate a tumor proliferative profile. They are responsible to create an environment conducive for immune suppression and cancer-induced immune tolerance[29]. The population of these cells in the tumor microenvironment of the treatment groups were also significantly affected showing the maximum decrease in the combination group followed by the PASA/DOX group (Figure 7. C)

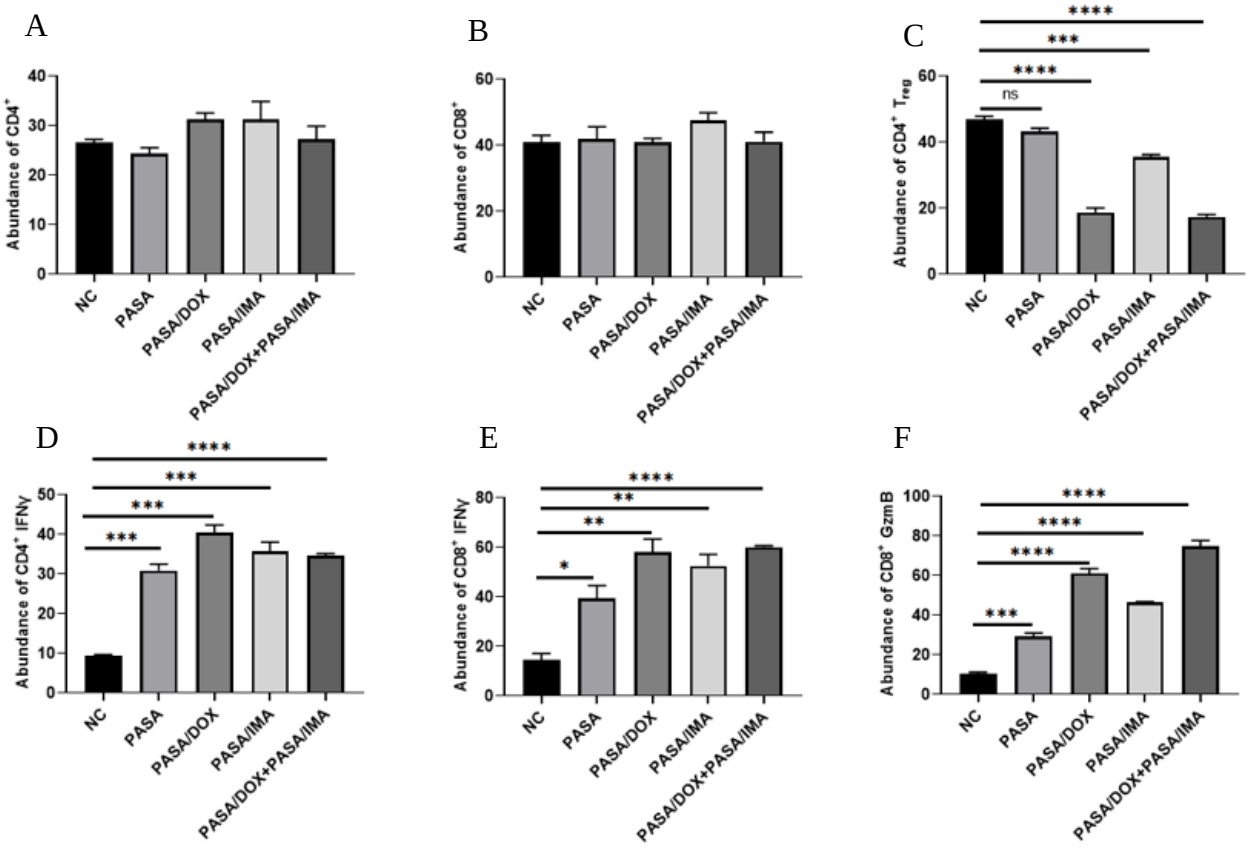

Figure 7: Changes in the CT26 tumor microenvironment

4.0 Conclusion

COX2 inhibition is an effective way to target the tumor microenvironment and suppress tumor growth[30]. The 5-ASA based polymer effectively incorporated DOX and IMA and formed stable micelles. Physicochemical characterization of the micelles suggested that they had ideal size, morphology, and stability characteristics. *In vitro* as well as *in vivo* studies demonstrated synergistic antitumor activity of free drugs as well as drug-loaded micelles in vitro and in vivo. The improved tumor immune microenvironment also contributed to the overall antitumor activity.

Our data also showed that DOX has the ability to decrease the expression of COX2 in the tumor cells in addition to a synergy with imatinib in inhibiting the proliferation of tumor cells. We hypothesize that the PASA polymer can inhibit the activity of the COX2 that has already been produced while DOX can help to inhibit the increased new synthesis of COX2 as a result of PASA-mediated inhibition of COX. Such a combination of imatinib-loaded PASA and DOX-loaded PASA can hence have a favorable anti-tumor therapeutic activity due to their synergistic action.

Appendix A : Abbreviations

TKI	Tyrosine kinase inhibitor
MDSC	Myeloid derived suppressive cells
DOX	Doxorubicin
IMA	Imatinib
COX	Cyclooxygenase
MDR1	Multidrug resistance protein 1
5-ASA	5-Acetyl salicylic acid
DMEM	Dulbecco's Modified Eagle's Medium
RPMI	Roswell Park Memorial Institute
FBS	Fetal bovine serum
AAALAC	Association for Assessment and Accreditation of Laboratory Animal Care
NMR	Nuclear magnetic resonance
PBS	Phosphate buffered saline
DLS	Dynamic light scattering
DLC	Drug loading capacity
DLE	Drug loading efficacy
qPCR	Quantitative polymerase chain reaction
SDS-PAGE	Sodium dodecyl sulphate- polyacrylamide gel electrophoresis
PVDF	Polyvinylidene difluoride
IgG	Immunoglobulin G
SEM	Standard error of mean

ANOVA	One-way analysis of variance
RAFT	Reversible addition-fragmentation chain-transfer
TEM	Transmission electron microscopy
IFNγ	Interferon γ
GzmB	Granzyme B
OD	Optical density

Appendix B : Chemicals

AIBN	2-Azobis-(isobutyronitrile)
PEG	Polyethylene glycol
MTT	3-(4,5-dimethylthiazol-2-yl)-2,5-diphenyl tetrazolium bromide
NHS	*N*-Succinimidyl Methacrylate
TEA	Triethylamine
DMSO	Dimethyl sulfoxide
DCM	Dichloromethane
ACN	Acetonitrile

Bibliography

1 Bellora, F. *et al.* Imatinib and Nilotinib Off-Target Effects on Human NK Cells, Monocytes, and M2 Macrophages. *The Journal of Immunology* **199**, 1516, doi:10.4049/jimmunol.1601695 (2017).

2 Iqbal, N. & Iqbal, N. Imatinib: a breakthrough of targeted therapy in cancer. *Chemother Res Pract* **2014**, 357027-357027, doi:10.1155/2014/357027 (2014).

3 Balachandran, V. P. *et al.* Imatinib potentiates antitumor T cell responses in gastrointestinal stromal tumor through the inhibition of Ido. *Nature Medicine* **17**, 1094-1100, doi:10.1038/nm.2438 (2011).

4 Li, C. & Han, X. Melanoma Cancer Immunotherapy Using PD-L1 siRNA and Imatinib Promotes Cancer-Immunity Cycle. *Pharmaceutical Research* **37**, 109, doi:10.1007/s11095-020-02838-4 (2020).

5 Seifert, A. M. *et al.* PD-1/PD-L1 Blockade Enhances T-cell Activity and Antitumor Efficacy of Imatinib in Gastrointestinal Stromal Tumors. *Clin Cancer Res* **23**, 454-465, doi:10.1158/1078-0432.Ccr-16-1163 (2017).

6 Cavnar, M. J. *et al.* KIT oncogene inhibition drives intratumoral macrophage M2 polarization. *J Exp Med* **210**, 2873-2886, doi:10.1084/jem.20130875 (2013).

7 Bertucci, F. *et al.* PDL1 expression is an independent prognostic factor in localized GIST. *OncoImmunology* **4**, e1002729, doi:10.1080/2162402X.2014.1002729 (2015).

8 Chen, Y., Sun, J., Huang, Y., Lu, B. & Li, S. Improved Cancer Immunochemotherapy via Optimal Co-delivery of Chemotherapeutic and Immunomodulatory Agents. *Molecular Pharmaceutics* **15**, 5162-5173, doi:10.1021/acs.molpharmaceut.8b00717 (2018).

9 Christiansson, L. *et al.* The Tyrosine Kinase Inhibitors Imatinib and Dasatinib Reduce Myeloid Suppressor Cells and Release Effector Lymphocyte Responses. *Molecular Cancer Therapeutics* **14**, 1181, doi:10.1158/1535-7163.MCT-14-0849 (2015).

10 Zitvogel, L., Rusakiewicz, S., Routy, B., Ayyoub, M. & Kroemer, G. Immunological off-target effects of imatinib. *Nature Reviews Clinical Oncology* **13**, 431-446, doi:10.1038/nrclinonc.2016.41 (2016).

11 Kreutzman, A., Porkka, K. & Mustjoki, S. Immunomodulatory Effects of Tyrosine Kinase Inhibitors. *International Trends in Immunity* **01** (2013).

12 Palamà, I. E., Cortese, B., D'Amone, S., Arcadio, V. & Gigli, G. Coupled delivery of imatinib mesylate and doxorubicin with nanoscaled polymeric vectors for a sustained downregulation of BCR-ABL in chronic myeloid leukemia. *Biomaterials Science* **3**, 361-372, doi:10.1039/C4BM00289J (2015).

13 Zhao, R. *et al.* PD-1/PD-L1 blockade rescue exhausted CD8+ T cells in gastrointestinal stromal tumours via the PI3K/Akt/mTOR signalling pathway. *Cell Proliferation* **52**, e12571, doi:10.1111/cpr.12571 (2019).

14 Cho, J. *et al.* Emergence of CTNNB1 mutation at acquired resistance to KIT inhibitor in metastatic melanoma. *Clinical and Translational Oncology* **19**, 1247-1252, doi:10.1007/s12094-017-1662-x (2017).

15 Tipping, A. J. & Melo, J. V. Imatinib mesylate in combination with other chemotherapeutic drugs: *In vitro* studies. *Seminars in Hematology* **40**, 83-91, doi:https://doi.org/10.1053/shem.2003.50047 (2003).
16 Fan, Y. *et al.* The reduction of tumor interstitial fluid pressure by liposomal imatinib and its effect on combination therapy with liposomal doxorubicin. *Biomaterials* **34**, 2277-2288, doi:https://doi.org/10.1016/j.biomaterials.2012.12.012 (2013).
17 Zhao, G., Sun, Y. & Dong, X. Zwitterionic Polymer Micelles with Dual Conjugation of Doxorubicin and Curcumin: Synergistically Enhanced Efficacy against Multidrug-Resistant Tumor Cells. *Langmuir* **36**, 2383-2395, doi:10.1021/acs.langmuir.9b03722 (2020).
18 Gupta, B. *et al.* Development of Bioactive PEGylated Nanostructured Platforms for Sequential Delivery of Doxorubicin and Imatinib to Overcome Drug Resistance in Metastatic Tumors. *ACS Applied Materials & Interfaces* **9**, 9280-9290, doi:10.1021/acsami.6b09163 (2017).
19 Chen, Y. *et al.* Co-delivery of doxorubicin and imatinib by pH sensitive cleavable PEGylated nanoliposomes with folate-mediated targeting to overcome multidrug resistance. *International Journal of Pharmaceutics* **542**, 266-279, doi:https://doi.org/10.1016/j.ijpharm.2018.03.024 (2018).
20 Sobolewski, C., Cerella, C., Dicato, M., Ghibelli, L. & Diederich, M. The role of cyclooxygenase-2 in cell proliferation and cell death in human malignancies. *Int J Cell Biol* **2010**, 215158-215158, doi:10.1155/2010/215158 (2010).
21 Liu, B., Qu, L. & Yan, S. Cyclooxygenase-2 promotes tumor growth and suppresses tumor immunity. *Cancer Cell International* **15**, 106, doi:10.1186/s12935-015-0260-7 (2015).
22 Arunasree, K. M. *et al.* Imatinib-resistant K562 cells are more sensitive to celecoxib, a selective COX-2 inhibitor: Role of COX-2 and MDR-1. *Leukemia Research* **32**, 855-864, doi:https://doi.org/10.1016/j.leukres.2007.11.007 (2008).
23 Dharmapuri, G., Doneti, R., Philip, G. H. & Kalle, A. M. Celecoxib sensitizes imatinib-resistant K562 cells to imatinib by inhibiting MRP1–5, ABCA2 and ABCG2 transporters via Wnt and Ras signaling pathways. *Leukemia Research* **39**, 696-701, doi:https://doi.org/10.1016/j.leukres.2015.02.013 (2015).
24 Markosyan, N. *et al.* Tumor cell–intrinsic EPHA2 suppresses antitumor immunity by regulating PTGS2 (COX-2). *The Journal of Clinical Investigation* **129**, 3594-3609, doi:10.1172/JCI127755 (2019).
25 Böttcher, J. P. *et al.* NK Cells Stimulate Recruitment of cDC1 into the Tumor Microenvironment Promoting Cancer Immune Control. *Cell* **172**, 1022-1037.e1014, doi:https://doi.org/10.1016/j.cell.2018.01.004 (2018).
26 Ritland, S. R. *et al.* Evaluation of 5-Aminosalicylic Acid (5-ASA) for Cancer Chemoprevention: Lack of Efficacy against Nascent Adenomatous Polyps in the Apc^{Min} Mouse. *Clinical Cancer Research* **5**, 855 (1999).
27 Huang, H. *et al.* A novel immunochemotherapy based on targeting of cyclooxygenase and induction of immunogenic cell death. *Biomaterials* **270**, 120708, doi:https://doi.org/10.1016/j.biomaterials.2021.120708 (2021).
28 Edwardson, D. W., Parissenti, A. M. & Kovala, A. T. in *Breast Cancer Metastasis and Drug Resistance: Challenges and Progress* (ed Aamir Ahmad) 173-215 (Springer International Publishing, 2019).

29 Larmonier, N. *et al.* Imatinib Mesylate Inhibits CD4⁺CD25⁺ Regulatory T Cell Activity and Enhances Active Immunotherapy against BCR-ABL[−] Tumors. *The Journal of Immunology* **181**, 6955-6963, doi:10.4049/jimmunol.181.10.6955 (2008).

30 Xu, L. *et al.* COX-2 Inhibition Potentiates Antiangiogenic Cancer Therapy and Prevents Metastasis in Preclinical Models. *Science Translational Medicine* **6**, 242ra284-242ra284, doi:10.1126/scitranslmed.3008455 (2014).